Biomimetic Centering Behavior

Mobile Robots with Panoramic Sensors

BY ANTONIS A. ARGYROS, DIMITRIS P. TSAKIRIS, AND CÉDRIC GROYER

In its continuous attempt to build intelligent artificial creatures, robotics has often been inspired by nature. Particularly interesting is the remarkable variety of light-sensing structures and information processing strategies occurring in animal visual systems. The physiology of these systems appears to have been influenced, through evolution, by the ecological niche and lifestyle of each animal species. Insects such as bees, ants, and flies have become a particularly appealing source of inspiration because of the remarkable navigational capabilities they display, despite their relatively restricted neural system. This, apparently, forced them to develop solutions to navigation tasks, which are ingenious in their simplicity and robust in their implementation, both of which are invaluable characteristics for robotic systems.

The navigation task examined in this work is the centering behavior, which consists of moving in the middle of a corridor-like environment. Bees are able to accomplish similar tasks by exploiting three features of their visuo-motor system: the wide field of view of their eyes, their ability to estimate retinal motion, and a control mechanism that reorients their flight so that retinal motion in the two eyes remains balanced [1].

Inspired by this biological solution, we attempt to create a reactive, vision-based centering behavior for a nonholonomic mobile robot equipped with a panoramic camera, providing a 360° visual field and a sensor-based control law, where optical flow information from several distinct directions in the entire field of view of the panoramic camera is used directly in the control loop. No reconstruction of the robot's state is attempted; the information extracted from the sensory data is not sufficient for this. It is, however, sufficient for the proposed control law to accomplish the desired task. The use of a panoramic camera, as opposed to that of a multicamera setup or of a mechanism that reorients the gaze of a typical perspective camera, simplifies the processing of the sensory information and reduces the complexity of the required hardware.

A detailed theoretical analysis, followed by extensive experimentation, demonstrates the effectiveness of this biologically motivated approach.

From Insects to Robots

Fundamental analogies exist between the behaviors that biological organisms and robots exhibit: mobile robots should be able to perceive the static and dynamic aspects of their environment and modify their behavior accordingly, very much like their biological counterparts. In insects, the centering behavior facilitates safe navigation by maximizing the animal's distance from surrounding obstacles. For the same reason, this type of behavior is important for robots, particularly those operating in man-made, indoor environments with many corridors and narrow passages through which the robot must safely navigate.

1070-9932/04/$20.00©2004 IEEE

Moreover, nature provides valuable hints for the design of the visual hardware that is appropriate for specific behaviors. Many insects have a pair of compound eyes that are immobile with respect to their body but provide a wide field of view, which compensates for their immobility. The simplicity of this visual system is evident if we compare it to the human one with its sophisticated eye movement system. Technologically, this capability can be implemented using panoramic cameras, which can provide a wide field of view to robots (up to 360°) [2]. By exploiting such cameras, a robot can observe most of its surroundings without the need for elaborate, human-like gaze control. An alternative would be to use perspective cameras and alter their gaze direction via pan-tilt platforms, manipulator arms, or spherical parallel manipulators. Another alternative would be to use a multicamera system in which cameras jointly provide a wide field of view. Both alternatives, however, may present significant mechanical, perceptual, and control challenges [3], [4]. Thus, panoramic cameras, which offer the possibility to switch the "looking direction" effortlessly and instantaneously, emerge as an advantageous solution. In current implementations of panoramic cameras, however, low resolution, in the sense of low visual acuity, is the price to pay for achieving panoramic vision. This reduced acuity could be a significant problem for tasks like fine manipulation. For navigation tasks, however, it seems that acuity could be sacrificed in favor of a wide field of view. For example, the estimation of three-dimensional (3-D) motion is facilitated by a wide field of view, because this removes the ambiguities inherent in this process when a narrow field of view is used [5].

Panoramic cameras offer a wide field of view and allow effortless and instantaneous switching of viewing directions, thus emerging as an effective sensor for several robot navigation tasks.

Insects possess a visual system that works fast and robustly to support navigation tasks, even though their brain has several orders of magnitude fewer neurons than the human brain. This seems to be due to the minimalist way they deal with 3-D vision problems and to the tight coupling of the motion pathway neurons to motor neurons. The compound eyes' properties do not allow them to infer depth reliably by binocular stereopsis or defocusing. It is image motion that appears to be the most significant cue in dealing with 3-D vision, and the compound eyes are especially suitable for detecting movement. Bees, for example, display the so-called centering response: while flying through narrow gaps, they tend to fly through the center of the gap, despite their lack of stereoscopic vision and their inability to explicitly estimate distance. The hypothesis put forward is that bees balance the image motion perceived by their two eyes; this was verified in corridors whose walls were lined with vertical black and white gratings [1].

We approach the robotic centering task in the way advocated by Purposive Vision [6], namely using information that is quite specific to it and, possibly, not general enough to support other behaviors; however, this particular behavior will be efficient and robust since it does not inherit the difficulties of solving a more complex problem, such as structure from motion, as an intermediate step. Certain physical characteristics of our system, like the panoramic sensor and the nonholonomic motion constraints, are related to the corridor-centering task and to the sensory data through retinal motion-based quantities; these quantities constitute a partial representation of the environment, sufficient only for the accomplishment of the task at hand and not for a full reconstruction of the environment's structure.

Previous robotic implementations of the centering behavior, which mostly do not employ panoramic cameras, are surveyed in [1] (see also related references in [4] and [7]). In [8], a mobile robot with two perspective cameras pointing laterally is used to implement a centering reflex by balancing the corresponding average optical flow fields using a proportional-integral-derivative (PID) controller. This is an approximate scheme, since it does not account for the influence of the robot's rotational motion on the measured optical flow. This problem is corrected in [9], where a trinocular camera system is employed. A camera pointing in the heading direction is used to compute a function of the rotational motion of the robot. This information is propagated to two peripheral cameras, which then isolate the translational component of the flow, necessary to implement accurately the centering behavior. This method employs normal flow, which can be robustly computed from the spatio-temporal derivatives of the image intensity function. Its disadvantage lies in the complexity of the trinocular visual system employed.

One of the few works where, to our knowledge, panoramic vision is used for the centering behavior is [1]. It is implemented through special V-shaped mirror arrangements, and the optical flow from the lateral directions is used to extract distance and orientation to the corridor walls, thus providing a complete reconstruction of the state of the robot. Similarly, [10] uses panoramic images to reconstruct the state of the robot via landmarks and uses this state in the path-following scheme developed in [11].

In [4], the use of a panoramic camera for the centering behavior is proposed. No state reconstruction is involved, since the panoramic flow is used to extract only a partial representation of the environment, useful for the task at hand. The paper presents a theoretical analysis of the stability of the resulting control law and provides simulation results. The present paper discusses extensive robotic experiments and demonstrates how the introduction of a panoramic camera simplifies both the hardware of the robotic system and the computational methods required for the processing of the

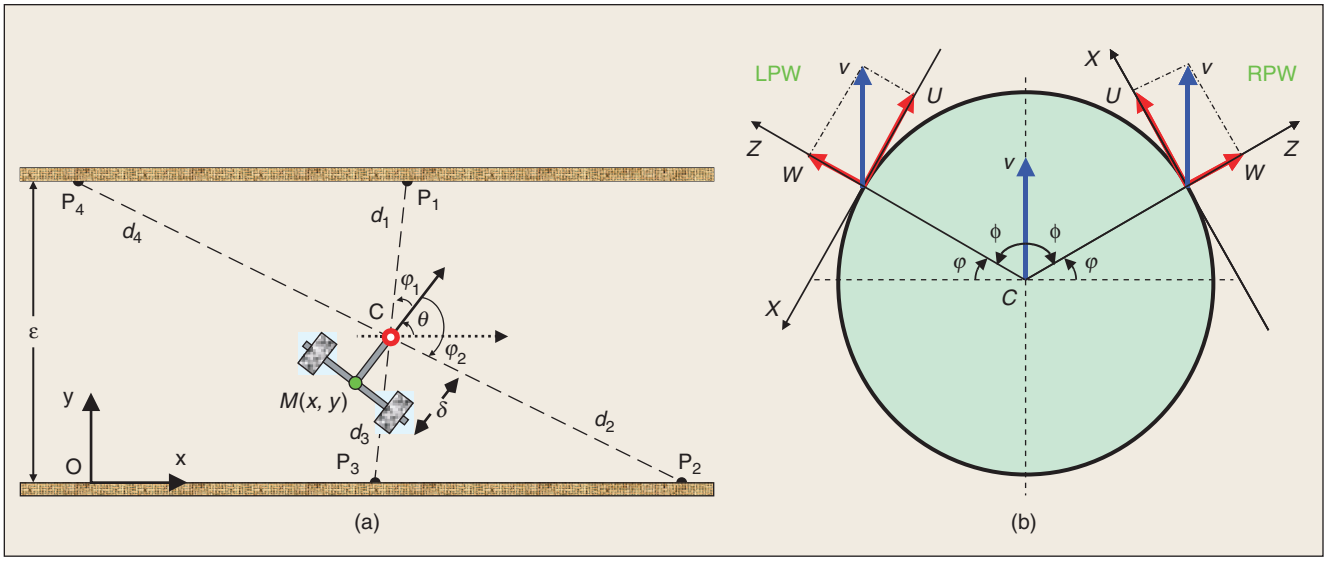

Figure 1. *(a) Model of a mobile robot with a panoramic camera. (b) The robot's translational velocity v is decomposed into a forward (W) and a lateral (U) translation in the local coordinate system of the virtual perspective cameras, which are located at viewing directions φ and $\pi - \varphi$.*

visual information. Furthermore, it extends the work presented in [4] by considering experiments with time-varying robot translational velocity and its adaptation to the corridor width, as well as the case of robot motion in a dynamic environment.

Extracting Information from Panoramic Data

We consider a mobile robot moving on a planar surface inside a corridor with straight parallel textured walls. The model of our system is shown in Figure 1(a). It includes an inertial coordinate system centered at a point O of the plane and aligned with one of the walls, a moving one attached to the middle M of the robot's wheel axis and another moving coordinate system attached to the point C where a panoramic camera is mounted. Let δ be the offset of the camera from the point M (i.e., the distance of the points C and M) and ε be the width of the corridor. With such a sensor configuration, the robot acquires panoramic views of its environment like the one shown in Figure 2(a).

Each acquired panoramic image can be unfolded by employing a polar-to-Cartesian transformation, giving rise to a cylindrical image [parts of such cylindrical images are shown in Figure 2(b) and (c)]. This transformation is computationally very efficient, since it involves only a look-up table operation. Different columns of the resulting cylindrical image correspond to different viewing directions in the range $[0, 2\pi]$. We assume that the heading direction of the robot is the one recorded on the cylindrical image column that corresponds to $\varphi = \pi/2$ [Figure 1(b)].

A cylindrical image can be approximated by a number of perspective images, which are tangent to the cylindrical surface and have no overlapping visual fields. As the number of perspective images increases, their corresponding horizontal visual fields become narrower and the approximation becomes more accurate. In the limit, these images become one dimensional (1-D) vertical stripes of pixels corresponding to the columns of the cylindrical image. For each of these images, we may employ the optical flow equations [12] to analyze the panoramic optical flow generated due to the robot's motion in a rigid environment. More specifically, consider the column of the cylindrical image that corresponds to the viewing direction φ. Suppose that the part of the 3-D scene projected on this column lays at depth d. The heading speed v of the robot can be decomposed in two components of translational velocity in the local image coordinate system of the virtual camera [Figure 1(b)]. The reorientation of the robot produces a rotational component of motion equal to the robot's angular velocity ω. In the notation of [12], $W = v \sin \varphi$, $U = v \cos \varphi$ and $\beta = \omega$. Then, the horizontal component of the optical flow in the viewing direction φ of the panoramic images is [4]:

Experiments with a mobile robot equipped with a panoramic camera, demonstrate an efficient and robust biomimetic centering behavior.

$$u_\varphi = \frac{vf \cos \varphi}{d} - \omega f. \tag{1}$$

Notice that the horizontal component of the optical flow u_{φ_h} in the heading direction φ_h is equal to $-\omega f$, i.e., it depends only on the rotational component of the robot's motion. Suppose now that we measure the horizontal component of the optical flow u_{φ_1} and u_{φ_2} in two different directions φ_1 and φ_2,

respectively, with corresponding depths d_1 and d_2. Define, then, the quantity $L_{1,2}$ as a function of the horizontal flow, as follows:

$$L_{1,2}(u) \triangleq u_{\varphi_1} + u_{\varphi_2} - 2u_{\varphi_h}. \tag{2}$$

This quantity is the sum of the horizontal flow in the directions considered, where the rotational component of the flow has been eliminated (derotation of the flow).The quantity $L_{1,2}$ can be expressed as a function of depth using (1). If the angles φ_1 and φ_2 are arranged symmetrically with respect to the heading direction $\varphi_h = \pi/2$ of the robot (i.e., if we choose an angle ϕ and set $\varphi_1 = \pi/2 + \phi$ and $\varphi_2 = \pi/2 - \phi$, with $\phi \in (0, \pi/2)$), we get

$$L_{1,2}(d) = vf \sin \phi \left(\frac{1}{d_1} - \frac{1}{d_2} \right). \tag{3}$$

Notice that, due to the derotation of the flow, the quantity $L_{1,2}$ is independent of the rotational velocity ω. Since φ_1 and φ_2 are directions symmetrical with respect to the heading direction, the aforementioned result states that, by computing $L_{1,2}$, the robot is able to perceive whether it is closer to obstacles to the left or to the right side of its heading direction, without actually computing explicitly the distances to these obstacles.

Since the computation of the quantity $L_{1,2}$ involves only the horizontal component of the optical flow, normal flow in selected edge directions (e.g., vertical edges) could have been used instead of optical flow, as in [9]. However, if normal flow is used, only a sparse subset of the image points could be used in the calculations. Even more importantly, a pyramidal optical flow computation scheme like the one used in this work permits the computation of flow corresponding to larger pixel displacements and increases the tolerance of the method to depth variations.

In order to implement the robot centering behavior, the optical flow is computed in three windows of the cylindrical image. The first window is centered at the heading direction and is used for computing u_{φ_h}. Computing u_{φ_h} by averaging the horizontal flow in a narrow window centered at the heading direction is an accurate enough approximation, necessary to ensure that, even in environments with relatively sparse texture, there will be enough optical flow vectors to enable a robust estimation of the rotational motion component. The flow u_{φ_h} is subsequently used [as indicated in (2)] to derotate the flow computed in two other windows, the left peripheral window (LPW) and the right peripheral window (RPW) where u_{φ_1} and u_{φ_2} are computed, respectively.

The location ϕ and the angular width of these windows are parameters

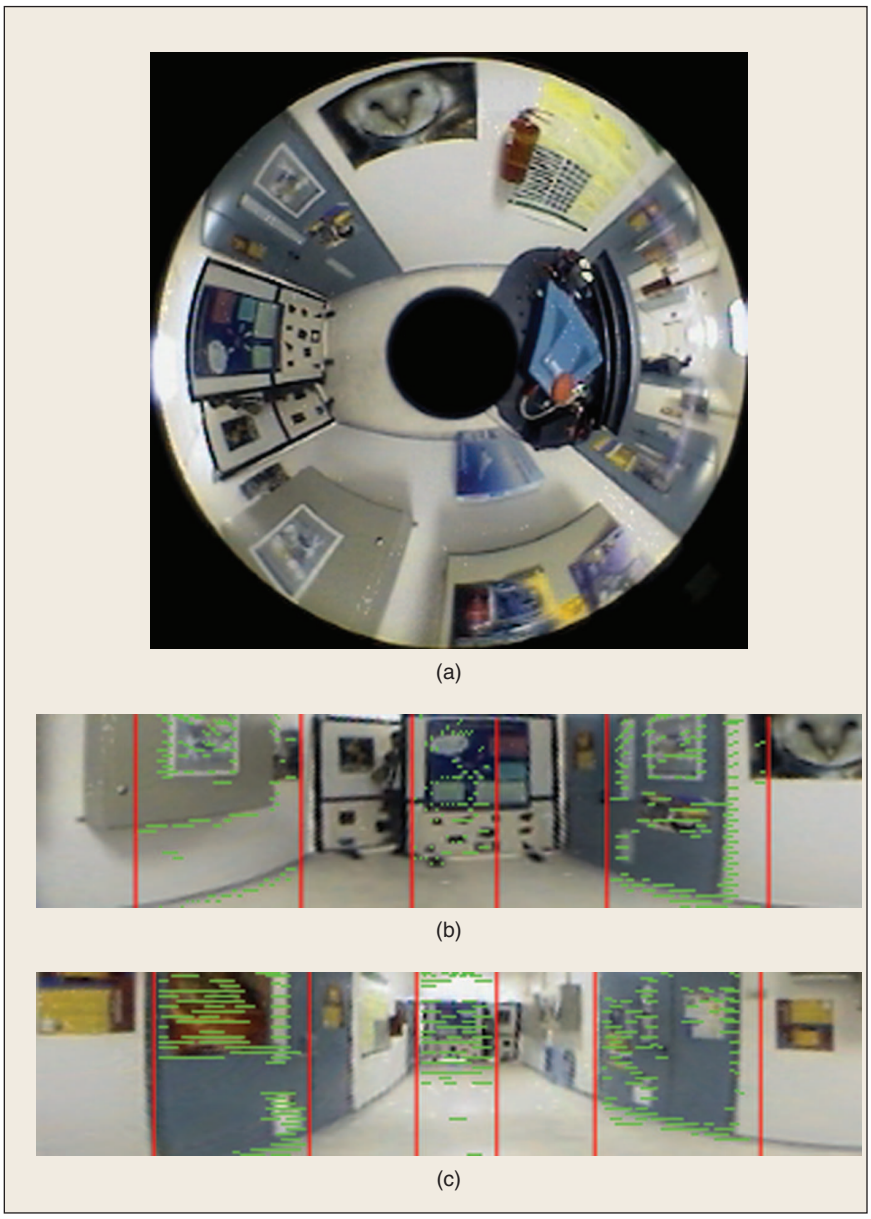

Figure 2. *(a) Sample panoramic image. (b) Example flow computation for the case of a robot moving straight in the middle of a corridor. (c) Same as in (b) for a robot translating and rotating close to the one of the walls of a corridor. Red vertical lines delineate the left, central, and right windows where flow is computed. The flow is superimposed on the visual data.*

that influence the resulting corridor following behavior. If ϕ is close to zero, the robot reacts to obstacles that are relatively far from its local environment. Moreover, sin ϕ is very close to zero and the contribution of the difference of inverse depths on $L_{1,2}$ is suppressed. If ϕ is close to $\pi/2$, then LPW and RPW are centered at a direction perpendicular to the heading direction. In this case, a control scheme based on $L_{1,2}$ would not correct heading errors, resulting in an oscillation around the middle of the free space [7], [9]. Setting ϕ around $\pi/4$ results in behaviors where the robot converges to the middle of the free space by following a smooth path.

The variation of the angular width of the LPW and RPW results in different degrees of reactivity with respect to the shape of the environment. If the windows are too wide, the local depth variations are suppressed and the robot reacts to the coarse shape characteristics of the environment. If the windows are too narrow, the robot becomes too sensitive to the local shape characteristics of it.

Figure 2(b) and (c) gives two examples of the process of extracting visual information from panoramic images towards supporting the corridor following behavior. In Figure 2(b), the computed optical flow is due to a forward translation of the robot in the middle of a corridor. As a result, the flow is balanced in the LPW and the RPW. In Figure 2(c) the robot translates and rotates close to the left wall of the corridor, therefore, the flow in the LPW and the RPW is not balanced. The effect of the robot reorientation is also evident in the central window.

Sensor-Based Control

In this section, a controller is designed that implements the corridor following behavior and is based on the intuitively appealing observation that the information contained in $L_{1,2}$ is sufficient for this task. Let (x, y) be the position of the point M and θ be the orientation of the mobile robot with respect to the inertial coordinate system. We will refer to (x, y, θ) as the state of the robot. We suppose that the wheels of the mobile robot roll without slipping on the plane supporting it. This imposes a constraint on the motion of the mobile robot, namely that the component of the instantaneous velocity, which is lateral to the heading direction of the robot, is always equal to zero. In mechanics, this is called a nonholonomic constraint; systems with such motion constraints have been widely studied in robotics because of the particular mechanical, control, and planning problems that arise [3], [4], [7], [11]. Then, we can model the mobile robot kinematics by the following set of nonlinear first-order ordinary differential equations (ODEs): $\dot{x} = \mathrm{v} \cos\theta$, $\dot{y} = \nu \sin\theta$, $\dot{\theta} = \omega$, where ν is the heading speed of the robot, defined as $\nu \triangleq \dot{x} \cos\theta + \dot{y} \sin\theta$ and ω is its angular velocity.

The task of following a straight-line corridor consists in using the angular velocity of the mobile robot to drive the lateral distance of the robot from the walls (y), as well as its orientation (θ), to desired values corresponding to the middle of the corridor. This goal can be expressed mathematically as the problem of asymptotically stabilizing the state of the (y, θ)-subsystem of the mobile robot kinematics (i.e., the last two of the previous system of ODEs) using only the angular velocity ω as the control of the system. We suppose that the heading speed ν is not explicitly controlled. Asymptotic stability of a system described by a set of (nonlinear) first-order ODEs means, on one hand, that arbitrarily small perturbations of its initial state from an equilibrium result in arbitrarily small perturbations of the corresponding trajectories and, on the other, that all trajectories starting sufficiently close to the equilibrium, eventually approach it as time tends to infinity. For more details on the stability concepts and methods used in this work, see [4] and [7].

When reconstruction of the state (y, θ) from the panoramic data is possible, a path-following control scheme (e.g., [11]) can be applied to the system, as in [10]. However, an alternative scheme is possible: the motion control scheme described in the following is based directly on the optical flow extracted from the panoramic image sequence. This accomplishes the desired task without the need for

Figure 3. *The mobile robot with a panoramic camera mounted on it. (a) The panoramic camera is centered on the robot's axis of rotation. (b) The panoramic camera is displaced significantly from the robot's axis of rotation.*

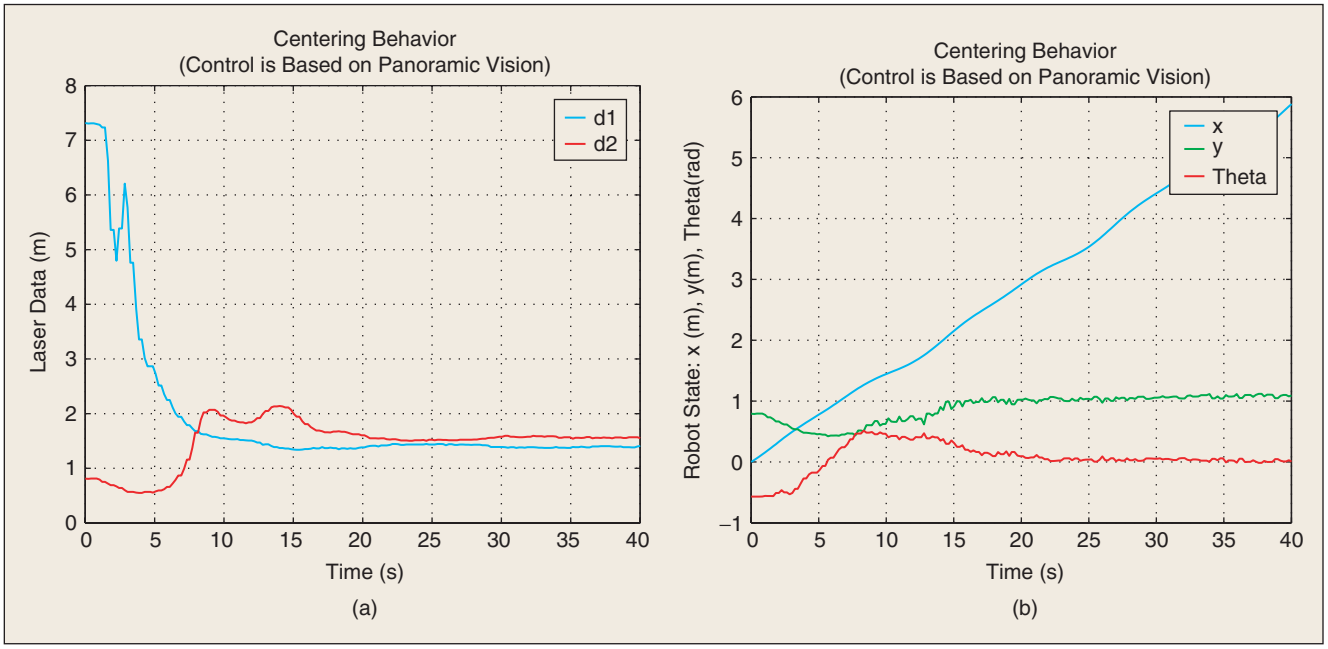

Figure 4. *Control based on vision. (a) Laser data d_1 and d_2. (b) State (x, y, θ) of the robot.*

reconstruction of the state from the panoramic data, which is usually a complicated and error-prone process.

In the case that v is time-varying, but strictly positive for all times (i.e., the robot continuously moves forward without stopping), the angular velocity control ω can use the quantity $L_{1,2}$ defined in (2), which is calculated by looking forward with the panoramic camera in three specific directions. It can be shown that this flow-based visual servoing control stabilizes locally and asymptotically the (γ, θ)-subsystem of the mobile robot kinematics to the middle of the corridor.

Let the heading speed v of the mobile robot be time varying and assume that it is strictly positive, piecewise continuous, and bounded at all times. Let the camera offset be $\delta \geq 0$. Assume further that the quantity $L_{1,2}$, defined as a function of optical flow in (2) in the three directions φ_h, $\varphi_1 = \pi/2 + \phi$ and $\varphi_2 = \pi/2 - \phi$, with $\phi \in (0, \pi/2)$, is related to the distances d_1 and d_2 as described in (3). Then, the angular velocity:

$$\omega(u) = -k\, L_{1,2}(u) = -k\, (u_{\varphi_1} + u_{\varphi_2} - 2u_{\varphi_h}), \qquad (4)$$

with gain $k > 0$, stabilizes locally asymptotically the (γ, θ)-subsystem of the mobile robot kinematics to the equilibrium $(\gamma_*, \theta_*) \equiv (\varepsilon/2, 0)$.

From the geometry of the setup of Figure 1(a), it is possible to express the distances d_i, $i = 1, 2$, as functions of the states γ and θ of the robot. Then, the control ω takes the form of a state-feedback control law and the previous proposition can be demonstrated using Lyapunov's indirect method. This is based on examining the properties of the linearization, around the desired equilibrium, of the nonlinear closed-loop system with state (γ, θ). For details on the proof, see [4] and [7].

From (3), the control of (4) can be expressed as a function of depth as

$$\omega(d) = -k\, v\, f\, \sin\phi \left(\frac{1}{d_1} - \frac{1}{d_2}\right). \qquad (5)$$

We will refer to (4) as the panoramic vision-based control law and to (5) as the inverse-depth control law. Notice that (5) contains the heading speed v explicitly, while (4), which is the focus of our study, does not.

When v is strictly negative, controlling the system by (4) will lead to instability, so a different control law is required. In this case, the angular velocity control should take into account two different peripheral windows located symmetrically to the direction opposite of the heading direction, i.e., by looking backwards. Moreover, when v is allowed to cross zero, we consider an angular velocity control ω that consists in switching appropriately between the two previous control laws by looking alternatively forward and backwards. This can be achieved easily with a panoramic camera [4].

Experiments

A series of experiments were performed at the Computational Vision and Robotics Laboratory (CVRL) of ICS-FORTH. The goal of these experiments was to test the behavior of the proposed panoramic vision-based control scheme and evaluate its performance in various corridor-following tasks.

The experiments were performed with the RWI B21r mobile robot of CVRL (Figure 3), which is equipped with a laser range finder and a Neuronics panoramic camera. The

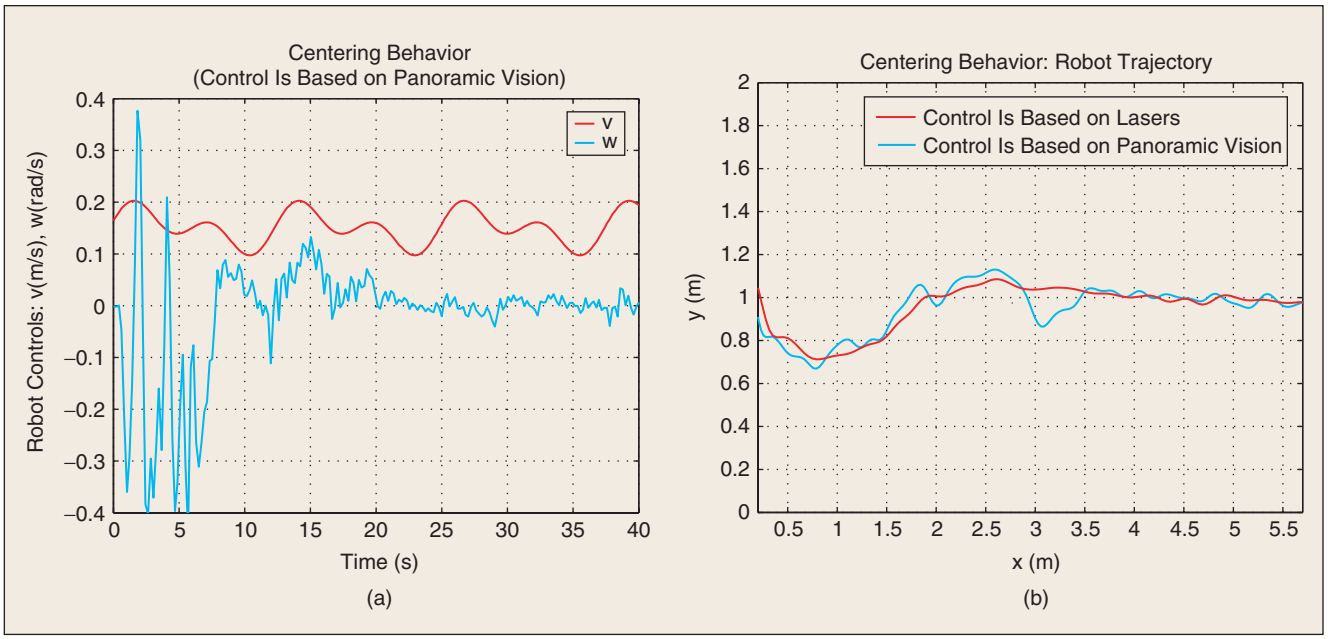

Figure 5. *(a) Robot heading speed v and angular velocity ω. (b) Trajectory (x, y) of the robot under control based on lasers versus trajectory under control based on panoramic vision.*

laser is used to provide ground truth, due to its increased accuracy compared to vision. It covers 180° of the robot's surroundings at an angular resolution of 0.5° and at a distance resolution of 5 cm. The panoramic camera is composed of a CCD camera with 8-mm focal length and a hyperboloidal mirror. Our models suppose that the optical axis of the camera is perpendicular to the ground plane and that the heading direction of the robot is known. However, these conditions are enforced in a rough, qualitative manner, not through an elaborate calibration procedure.

In order to support processing of sensory information and the control of the platform, the robot is equipped with two Pentium III computers running at 800 MHz. Sensory information processing involves the unwrapping of the panoramic images to cylindrical ones, the definition of the LPW, the RPW, and the central window, the optical flow computation through the Lucas-Kanade method [13] and the computation of the angular velocity control. The duration of this cycle of operations is approximately 200 ms. Small variations of the duration of each cycle are due to the varying number of optical flow vectors employed in the three windows, as a result of texture variations in the scene. In all reported experiments, the panoramic flow u_{φ_h} is computed within a window of 15° centered at the heading direction, while the panoramic flows u_{φ_1} and u_{φ_2} are computed within windows (LPW and RPW) located at ±45° with respect to the heading direction and having an angular width of 30°. The locations and sizes of these windows were determined experimentally. The laser data d_1 and d_2 are acquired in directions ±45° with respect to the robot heading.

In the first of the reported experiments, the robot moves in a straight corridor, approximately 2.15 m wide ($\varepsilon \approx 2.15$ m), whose walls are covered with nonuniform color texture. It starts at the initial configuration $(y, \theta) = (0.80\text{ m}, -0.57\text{ rad})$ and reaches the final configuration $(y_*, \theta_*) = (1.1\text{ m}, 0\text{ rad})$, while moving forward with a preset, time-varying heading speed given by $v(t) = 0.15 + 0.03\sin(0.5t) + 0.03\sin(t)$ m/sec. The rotational motion of the robot is determined by the control law of (4) with gain $k = 0.5$. Increasing the gain k makes the robot more reactive, but its trajectory becomes more oscillatory. Figures 4 and 5 show experimental results from the robot moving under this control law. Figure 4(a) shows the corresponding laser data d_1 and d_2, while Figure 4(b) shows the state (x, y, θ) of the robot, which is reconstructed from the laser data [7]. These state estimates are not used in controlling the robot, they only indicate ground truth, which is used to quantify the behavior of the system. We observe that the distances from the walls converge towards the same value, designating motion of the robot in the middle of the corridor. However, a small error remains [Figure 4(a)], which is due to the errors in the optical flow computation and the derotation processes.

Figure 5(a) shows the angular velocity control ω and the translational velocity v of the robot. Small-amplitude variations in ω are mainly due to noise in the visual data. Since they are mostly damped by the mechanical properties of the system, no additional filtering of ω is performed. Thus, the robot (x, y)-trajectory appears quite regular [blue line in Figure 5(b)]. The second trajectory [red line in Figure 5(b)] is obtained when the robot is controlled using laser data via the control law of (5) (i.e., under "perfect" sensory information). It is clear that there is a close match between the two trajectories.

Figure 6(a) shows graphically the robot location and orientation during this corridor-following experiment. Figure 6(b) presents snapshots of this experiment, acquired by an external observer. The initial robot position is close to the right wall of the corridor and its initial heading direction is towards this

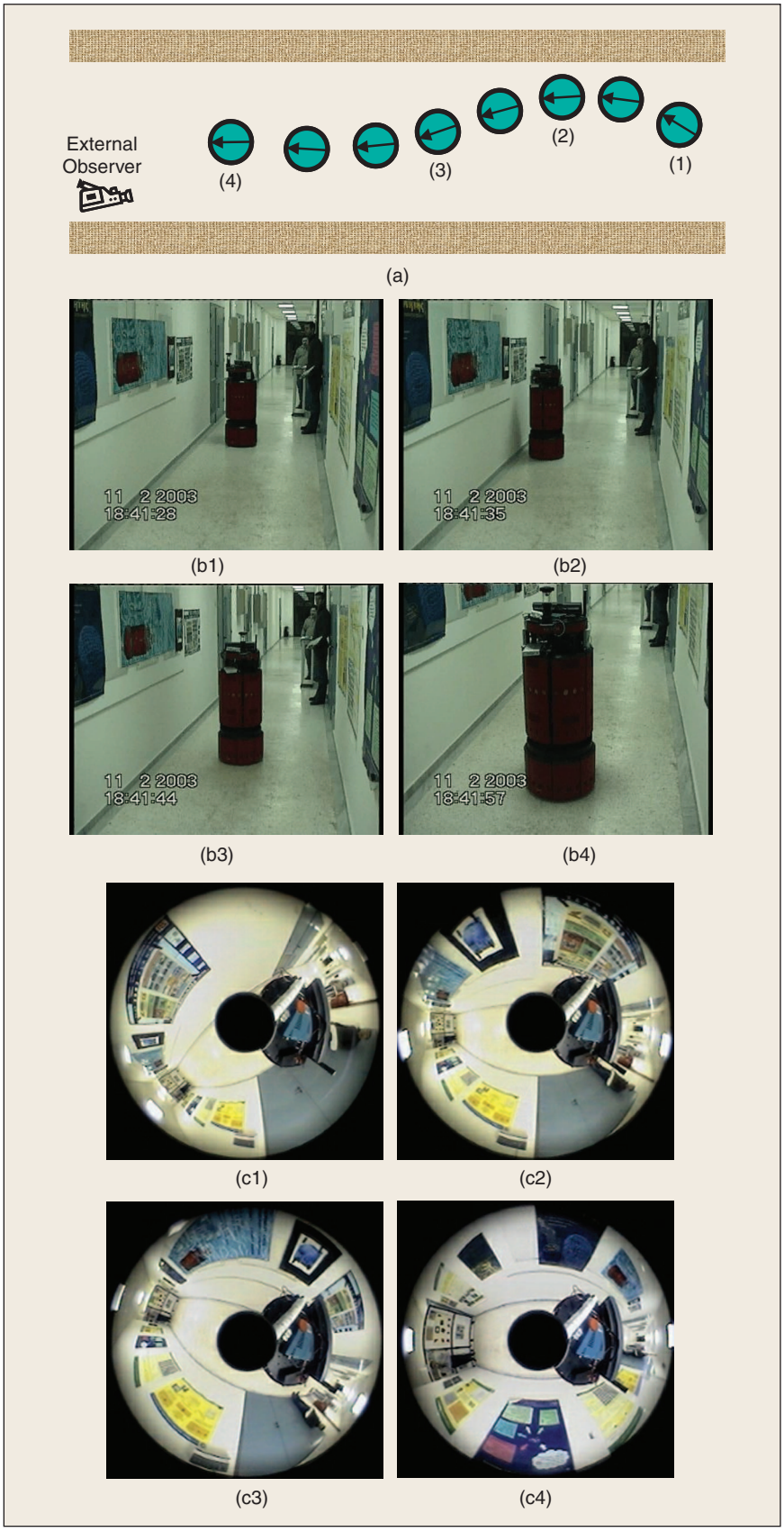

Figure 6. *Experiments with the centering behavior in a straight corridor. (a) Robot positions during the experiment. (b) Snapshots of the behavior as seen by an external observer at robot positions 1–4. (c) Panoramic views acquired by the robot at these positions.*

wall. As the experiment proceeds, the robot is gradually converging to the middle of the corridor and its pose becomes parallel to the walls. Figure 6(c) presents sample panoramic images that the robot acquired during this same experiment. Numerical labels at the robot positions in Figure 6(a) are in correspondence with numerical labels in Figures 6(b) and 6(c).

Experiments of the type described previously were performed successfully with the panoramic camera both centered on the robot axis [$\delta = 0$ in Figure 1(a), as in Figure 3(a)] and uncentered [$\delta > 0$, as in Figure 3(b)]. In the experiments of Figures 4 and 5, the offset δ is approximately 25 cm. Our experimental results demonstrate that the overall control scheme is robust to such modeling errors.

Experiments in more complicated environments established the wider interest of this class of panoramic vision-based control schemes, in particular in traversing corridors of varying widths, corridors containing static obstacles, and corridor-like spaces of more complex shape (e.g., curved, with angles, etc.). Several such experiments have been conducted; Figure 7 shows snapshots of a representative example, in which the robot moves in a Γ-shaped corridor. As these snapshots demonstrate, the robot is able to react appropriately to the more complex shape of this environment and stay in the middle of the free space.

In both previous experiments, the translational velocity of the robot was preset (time-varying in the experiment of Figure 6, constant in the experiment of Figure 7). Another class of experiments considers a robot moving in a corridor of varying width, shown graphically in Figure 8(a). Unlike the previous two experiments, the translational velocity of the robot is also controlled, adapting to the average flow in the two side windows. More specifically, the control $\dot{v}(t) = -k_1(u_{\varphi_1} - u_{\varphi_2} - u_*)$ is used to adapt the translational velocity of the robot to the width of the corridor [1], [8]. In this control law, u_* is a reference flow value that is chosen experimentally and k_1 is a positive gain. Related experimental results are shown in Figure 8, with $u_* = 1.0$ and $k_1 = 0.01$. The angular

velocity ω is controlled as in the previous experiments. Figure 8(b) shows, on the same plot, the robot's translational velocity (v) and the width (ε) of the corridor, both of which vary with time. For illustration purposes, the translational velocity was multiplied by a factor of five. It is evident that the robot increases its speed in the wide parts of the corridor and reduces it in the narrow parts.

The proposed robot-centering behavior is based on the assumption that the robot moves in a static environment. The presence of independently moving objects, visible in the parts of the panoramic images that are used for extracting flow information, affect the behavior of the robot. Several experiments have been carried out in corridors containing moving objects. When a moving object translates in the same direction as the robot, the relative retinal motion of the object and the robot decreases, as if the object had moved further away. The robot then rotates towards the object, in an effort to balance the retinal flow. Analogously, if the moving object translates in a direction opposite to that of the robot, the robot rotates away from the object. In both cases, balancing the flow results in a movement of the robot along the middle of the perceived free space, not along the middle of the real free space between the obstacle and the corridor walls. This result is consistent with observations regarding bee response to moving wall texture [1].

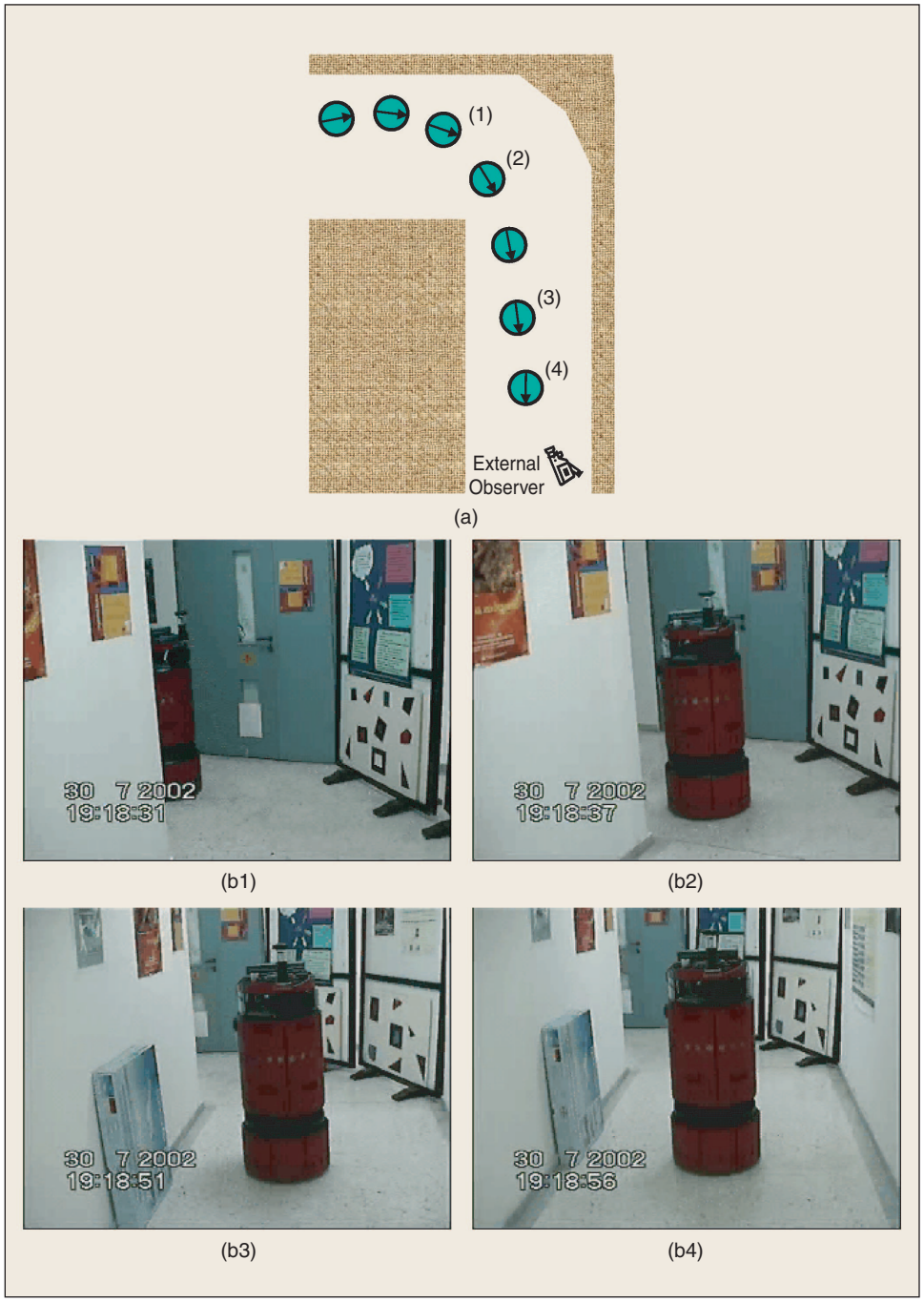

Figure 7. *Centering behavior in a Γ-shaped corridor. Letter captions in (b) roughly correspond to the enumeration of robot positions in (a).*

Videos of related experiments can be found in http://www.ics.forth.gr/cvrl/demos.

Conclusions

A reactive robotic centering behavior based on panoramic vision has been presented, which is inspired by the way insects exploit visual information in analogous navigation tasks. By employing a panoramic camera, the development of the centering behavior is simplified both from a theoretical and from an implementation point of view. The proposed method relies on the extraction of primitive visual information from appropriately selected areas of a panoramic visual field and its direct use in the control law. Experimental results from an implementation of this method on a robotic platform demonstrate a centering behavior which can be achieved in real-time and with high accuracy. The proposed technique circumvents the need to address complex problems of 3-D structure estimation and the resulting control laws were shown to possess the required stability properties.

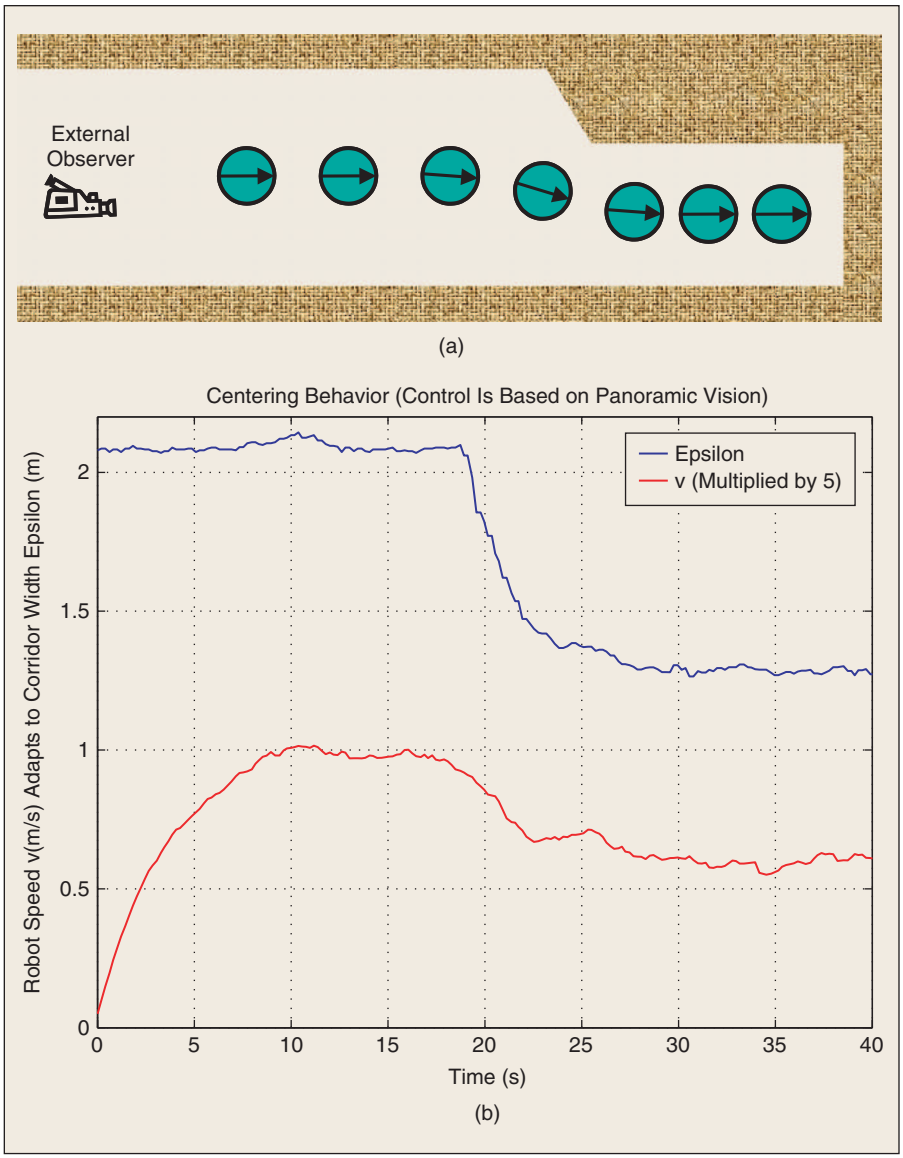

Figure 8. *Experiments in a corridor of varying width, where the translational velocity of the robot adapts to the width of the corridor based on panoramic flow information.*

Future research aims at extending this class of visual servoing schemes to more complex robot dynamics (e.g., flying robots) and at studying analogous principles for other complex navigation behaviors, like robot homing.

Acknowledgments

This work has been partially financially supported by the EU-IST Projects TOURBOT (IST-1999-12643), WebFAIR (IST-2000-29456) and BIOLOCH (IST-2001-34181). The authors would like to acknowledge insightful discussions with the members of the CVRL group of ICS-FORTH and the constructive criticism of the reviewers.

Keywords

Panoramic vision, biomimetic robotics, visual servoing, centering behavior, corridor-following, nonholonomic mobile robots.

References

[1] M.V. Srinivasan, J.S. Chahl, K. Weber, S. Venkatesh, M.G. Nagle, and S.W. Zhang, "Robot navigation inspired by principles of insect vision," *Robot. Autonom. Syst.*, vol. 26, no. 2–3, pp. 203–216, 1999.

[2] R. Benosman and S.B. Kang, Eds., *Panoramic Vision*. New York: Springer-Verlag Inc., 2001.

[3] D.P. Tsakiris, P. Rives, and C. Samson, "Extending visual servoing techniques to nonholonomic mobile robots," in *The Congruence of Vision and Control*, G. Hager, D. Kriegman, and S. Morse, Eds. (Lecture Notes in Control and Information Systems (LNCIS 237)). New York: Springer-Verlag, 1998.

[4] D.P. Tsakiris and A.A. Argyros, "Corridor Following by Nonholonomic Mobile Robots Equipped with Panoramic Cameras," in *Proc. 8th IEEE Med. Conf. Control Automation (MED2000)*, P.P. Groumpos, N.T. Koussoulas, and P.J. Antsaklis, Eds., Rio, 2000.

[5] C. Fermüller and Y. Aloimonos, "Geometry of Eye Design: Biology and Technology," in *Multi-Image Analysis*, R. Klette, T.S. Huang, and G.L. Gimel'farb, Eds. (Lecture Notes in Computer Science 2032). New York: Springer, pp. 22–38, 2001.

[6] Y. Aloimonos, Ed., *Active Perception*. Hillsdale, NJ: Lawrence Erlbaum Assoc., 1993.

[7] D.P. Tsakiris, A.A. Argyros, and C. Groyer, "Experiments in corridor following with nonholonomic mobile robots equipped with panoramic cameras," *Institute of Computer Science—FORTH*, Tech. Rep. FORTH-ICS TR-318-2003, 2003.

[8] J. Santos-Victor, G. Sandini, F. Curotto, and S. Garibaldi, "Divergent stereo in autonomous navigation: From bees to robots," *IJCV*, vol. 14, no. 1, pp. 159–177, 1995.

[9] A.A. Argyros and F. Bergholm, "Combining central and peripheral vision for reactive robot navigation," in *Proc. CVPR'99, Fort Collins, CO*, 1999, pp. 2646–2651.

[10] J. Gaspar and J. Santos-Victor, "Visual path following with a catadioptric panoramic camera," in *Proc. 7th Intl. Symp. on Intel. Robot. Syst. (SIRS'99)*, Coimbra, 1999, pp. 139–147.

[11] C. Samson, "Control of chained systems: Application to path following and time varying point-stabilization of mobile robots," *IEEE Trans. Automat. Contr.*, vol. 40, no. 1, pp. 64–77, 1995.

[12] B.K.P. Horn, *Robot Vision*. New York: McGraw-Hill, 1986.

[13] B.D. Lucas and T. Kanade, "An iterative image registration technique with an application to stereo vision," in *Proc. IJCAI'81*, Vancouver, BC, pp. 674–679, 1981.

Antonis A. Argyros is a research scientist at the Institute of Computer Science (ICS) of the Foundation for Research and Technology (FORTH) in Heraklion, Crete, Greece. He received his Ph.D. from the Department of Computer

(continued on page 68)

same institution. His research interests include distributed robot control strategies, probabilistic algorithms for automated navigation/localization, visual feature-detection algorithms for servoing applications, human/robot interfaces, and development of real-time algorithms for embedded control systems. He is a Member of the IEEE, ACM, and AAAI.

Nikolaos P. Papanikolopoulos received the Diploma degree in electrical and computer engineering from the National Technical University of Athens, Athens, Greece, in 1987, the M.S.E.E. in electrical engineering from Carnegie Mellon University (CMU), Pittsburgh, Pennsylvania, in 1988, and the Ph.D. in electrical and computer engineering from Carnegie Mellon University, Pittsburgh, Pennsylvania, in 1992. Currently, he is a professor in the department of computer science at the University of Minnesota and director of the Center for Distributed Robotics. His research interests include robotics, sensors for transportation applications, control, and computer vision. He has authored or coauthored more than 170 journal and conference papers in these areas (41 refereed journal papers). He was finalist for the Anton Philips Award for Best Student Paper in the 1991 IEEE Int. Conf. on Robotics and Automation and recipient of the best Video Award in the 2000 IEEE Int. Conf. on Robotics and Automation. He was recipient of the Kritski fellowship in 1986 and 1987. He was a McKnight Land-Grant Professor at the University of Minnesota for the period 1995-1997, and has received the NSF Research Initiation and Early Career Development Awards. He was also awarded the Faculty Creativity Award from the University of Minnesota. One of his papers (co-authored by O. Masoud) was awarded the IEEE VTS 2001 Best Land Transportation Paper Award. He has also received grants from DARPA; Sandia National Laboratories; NSF; Microsoft; INEEL; USDOT, DHS, and Air Force; MN/DOT; Honeywell; and 3M.

Address for Correspondence: Nikos Papanikolopoulos, Department of Computer Science and Engineering, University of Minnesota, Minneapolis, MN 55455 USA. E-mail: npapas@cs.umn.edu.

Biomimetic Centering Behavior

BY ANTONIS A. ARGYROS, DIMITRIS P. TSAKIRIS, AND CÉDRIC GROYER

(continued from page 30)

Science, University of Crete, Greece, in visual motion analysis. He has been a postdoctoral fellow at the Royal Institute of Technology in Stockholm, Sweden, where he worked on vision-based, reactive robot navigation. In 1999 he joined the Computational Vision and Robotics Laboratory of ICS-FORTH, where he has been involved in many RTD projects in image analysis, computational vision and robotics. His current research interests include computational vision and robotics and particularly the visual perception of motion and 3-D structure, the development of robot behaviors based on visual information and alternative visual sensors.

Dimitris P. Tsakiris is a research scientist at the Institute of Computer Science of FORTH and a visiting professor at the University of Crete. He received his B.S. degree from the Department of Electrical Engineering of the National Technical University of Athens and his M.S. and Ph.D. degrees from the Department of Electrical Engineering of the University of Maryland at College Park. Prior to his current position, he was a Marie Curie postdoctoral fellow in INRIA, Sophia-Antipolis. His research interests lie in the areas of sensor-based robotics, nonlinear control, undulatory locomotion, geometric mechanics, and computational vision. He is a principal investigator and coinvestigator of several European IST projects and research networks related to these research areas.

Cédric Groyer is a research and development engineer at the Computational Vision and Robotics Laboratory of ICS/FORTH. He received his B.Sc. degree in École Nationale Supérieure de Physique de Marseille, with major in Signal Processing. His interests include image processing and computer vision, with emphasis on their application to mobile robotics.

Address for Correspondence: Dimitris P. Tsakiris, Institute of Computer Science-FORTH, Vassilika Vouton, P.O. Box 1385, GR-71110 Heraklion, Greece. Tel.: +30 2810 391708. Fax: +30 2810 391601. E-mail: tsakiris@ics.forth.gr. URL: http://www.ics.forth.gr/~tsakiris.